molecular pharmaceutics

ACS Editors' Choice

Article

pubs.acs.org/molecularpharmaceutics

Immunocompetent 3D Model of Human Upper Airway for Disease Modeling and In Vitro Drug Evaluation

Helen Harrington,[†] Paul Cato,[†] Fabian Salazar,[†] Malcolm Wilkinson,[‡] Alan Knox,[§] John W. Haycock,[⊥] Felicity Rose,[¶] Jon W. Aylott,[¶] and Amir M. Ghaemmaghami*[,†]

[†]Division of Immunology, School of Life Sciences, Faculty of Medicine & Health Sciences, University of Nottingham, Nottingham NG7 2UH, United Kingdom

[‡]Kirkstall Ltd, Centurion Business Park, Templeborough, Rotherham, South Yorkshire S60 1FB, United Kingdom

[§]Division of Respiratory Medicine, Nottingham City Hospital, School of Medicine, University of Nottingham, Nottingham NG5 1PB, United Kingdom

[⊥]Kroto Research Institute, Dept. Materials Science & Engineering, University of Sheffield, Sheffield, South Yorkshire S3 7HQ, United Kingdom

[¶]School of Pharmacy, University of Nottingham, Nottingham NG7 2RD, United Kingdom

ABSTRACT: The development of more complex in vitro models for the assessment of novel drugs and chemicals is needed because of the limited biological relevance of animal models to humans as well as ethical considerations. Although some human-cell-based assays exist, they are usually 2D, consist of single cell type, and have limited cellular and functional representation of the native tissue. In this study, we have used biomimetic porous electrospun scaffolds to develop an immunocompetent 3D model of the human respiratory tract comprised of three key cell types present in upper airway epithelium. The three cell types, namely, epithelial cells (providing a physical barrier), fibroblasts (extracellular matrix production), and dendritic cells (immune sensing), were initially grown on individual scaffolds and then assembled into the 3D multicell tissue model. The epithelial layer was cultured at the air−liquid interface for up to four weeks, leading to formation of a functional barrier as evidenced by an increase in transepithelial electrical resistance (TEER) and tight junction formation. The response of epithelial cells to allergen exposure was monitored by quantifying changes in TEER readings and by assessment of cellular tight junctions using immunostaining. It was found that epithelial cells cocultured with fibroblasts formed a functional epithelial barrier at a quicker rate than single cultures of epithelial cells and that the recovery from allergen exposure was also more rapid. Also, our data show that dendritic cells within this model remain viable and responsive to external stimulation as evidenced by their migration within the 3D construct in response to allergen challenge. This model provides an easy to assemble and physiologically relevant 3D model of human airway epithelium that can be used for studies aiming at better understanding lung biology, the cross-talk between immune cells, and airborne allergens and pathogens as well as drug delivery.

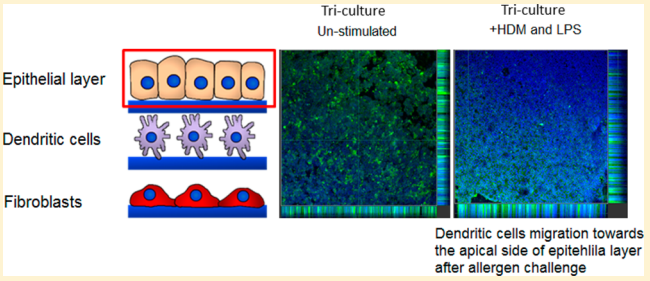

KEYWORDS: *Lung, 3D scaffold, coculture, triculture, immune cells, electrospinning, dendritic cells, allergy*

INTRODUCTION

Respiratory diseases such as asthma are becoming increasingly prevalent, with reduced longevity and quality of life for those affected as well as causing an economic burden upon healthcare systems worldwide.[1] Consequently, there is a need to develop more effective therapies to prevent and treat respiratory diseases. Developing new therapies requires extensive testing to ensure efficacy and safety, which is both time-consuming and costly. Therapies that show promise during the first stage preclinical in vitro tests may be taken forward for further studies. For all new medications, regulatory authorities insist upon acquiring information from animal studies because the effect upon the whole body can be observed. However, the limited biological relevance of animal models to human diseases means that data obtained from such studies could not always be relied on.

In vitro models of human tissues that are biomimetic and closely represent the functional properties of their respective tissues could enable better understanding of disease processes, hence providing more physiologically relevant platforms for identification of targets for therapy as well as testing the efficacy

Special Issue: Engineered Biomimetic Tissue Platforms for in Vitro Drug Evaluation

Received: January 12, 2014
Revised: March 9, 2014
Accepted: March 14, 2014
Published: March 14, 2014

and safety of new drug leads. Using such in vitro models in drug discovery cycle could in turn substantially reduce the number of drug leads that need to be taken forward to preclinical studies and, therefore, reducing the number of animals required for such experiments.[2] In addition to providing scientific advantages (e.g., identification of more efficacious targets for therapy), using biomimetic in vitro tissue models also conforms with the "3Rs" principles of refinement, replacement, and reduction of animal experimentations in research wherever possible.[3]

The respiratory system is constantly exposed to potentially harmful particles, allergens, and pathogens. To maintain sterility of the lung the respiratory system has a series of defense mechanisms and the capability to respond to environmental challenges. Epithelial cells are the predominant cell type in contact with the air and as such the airway epithelium forms the first line of defense against airborne insults. Epithelial cells are structurally arranged to form a continuous layer and are joined via protein junctions to create a paracellular barrier to shield interstitial tissue from the airway. As well as a physical barrier, the epithelium forms a chemical barrier via cellular secretions, for example, mucus that entraps infiltrating particles. Furthermore, contact with invading pathogens prompts epithelial cells to release lysozymes and phospholipase that destabilize bacterial membranes, defensins that have antimicrobial activity, and surfactants that promote phagocytosis of invading particles.[4]

If the epithelial barrier is compromised, the epithelial cells not only change morphologically and functionally but also communicate reciprocally via paracrine[5] or contact-dependent signaling with other cell types, such as underlying stromal and immune cells including macrophages, DCs, lymphocytes, neutrophils, and mast cells.[6,7] Summoning support from underlying cells can assist in restoring the epithelial barrier or initiate an immune response through expression of adhesion molecules and release of mediators including cytokines and chemokines.[4] The synergistic interactions of cells within human lung tissue remains largely understudied; in particular, few in vitro lung models report the inclusion of immune cells that are essential for sensing cellular and environmental changes as well as exerting a crucial role in the pathogenesis of lung diseases. The tissue engineering of lung models has largely focused toward engineering tracheal replacements due to the simpler nature of this tissue.[8] The robust architecture of the trachea can withstand the decellularization process and subsequent repopulation, whereas it proves difficult to repopulate decellularized tissue from deeper within the lung that has a more complex construction. The specific structural and cellular architecture of complex lung tissue can be retained for experimentation by using ex vivo tissue explants. These biopsy samples are practical for short-term experimentation, though interindividual variability can have an impact upon the results and the availability of such tissue is limited. To allow high-throughput screening of samples and, particularly, longer-term experiments, it is preferable to have a sustainable source of reproducible tissue models.

The use of commercially available two-dimensional (2D) platforms upon which epithelial cells can be cultured at the air−liquid interface (ALI) is widely practiced. Although information regarding cellular interaction can be identified using these methods, the 2D platforms fail to represent the cellular arrangement seen in vivo and, therefore, are not amenable to direct cell−cell interaction, thus only permitting observation of paracrine interactions. The use of a 3D tissue equivalent is favorable over 2D cell culture providing more in-vivo-like morphology, function, and intercellular interactions enabling greater resemblance to physiological conditions.[9,10] Encapsulating cells within synthetic or natural hydrogels has been widely used for culturing cells in a 3D environment and provide greater cell−cell contact compared to culturing upon a solid 2D substrate.[11] In addition, hydrogels could provide a cellular microenvironment resembling the native extracellular matrix (ECM), hence supporting key functional properties of different cell types.[12,13] Although many cell types seem to thrive within the 3D environment of hydrogels, encapsulating epithelial cells whose primary function is barrier formation could be counterintuitive. Therefore, other types of 3D matrix such as porous fiber sheets could be a favorable alternative for culturing epithelial cells, providing closer morphological resemblance to the basement membrane in barrier tissues such as skin and respiratory epithelium.[14] Obviously, this does not preclude use of hydrogel based scaffolds with the optimal topography for 3D culture of epithelial cells.

Methods to create fibrous 3D platforms include phase separation,[15] electrospraying,[16] or electrospinning.[17] We show that the ECM of lung tissue has a randomly arranged network of nanometer-sized fibers, and as such, the electrospinning method proves a suitable choice to create a matrix that mimics this arrangement for culturing lung associated cells. The porous network of polymer fibers that is produced can be tailored in morphology and dimensions to mimic the native ECM of the cells being cultured. Electrospun scaffolds may be constructed from a plethora of materials. Although there has been some success in the construction of pure protein electrospun scaffolds (e.g., collagen[18] and fibrinogen[19]), poor structural strength limits their use. Synthetic polymers offer the choice of well-defined batches with a greater range of mechanical and chemical properties than those of natural materials. Furthermore, synthetic polymers may adsorb ECM proteins in solution or can be surface modified for enhanced cell attachment if necessary.[14,20] Synthetic polymers PLA and PLGA are the more extensively studied, having been explored for both in vitro[21] and in vivo research.[22] However, PLA and PLGA are biodegradable and, in our preliminary experiments, were found to become quite fragile and difficult to handle after few days of cell culture, hence proving unsuitable to support long-term cell cultures for the 3D lung model. Thus, use of other nonbiodegradable and biologically nonfouling polymers such as poly(ethylene terephthalate) (PET), which was reported to support cell culture, was considered.[23]

Subsequently, in this study, we have used electrospun fibers of PET to create a 3D model of airway epithelium, comprising epithelial cells, dendritic cells, and fibroblasts, cultured at ALI. The model has been characterized with regards to its barrier function, responses to environmental stimuli, and migratory properties of the immune cells after allergen challenge.

This model possesses reasonable cellular and structural representation of the airway epithelium and is amenable to in situ monitoring, and as such, it presents an invaluable tool for academic and pharmaceutical research within the fields of lung biology, disease modeling, and drug discovery and delivery.

EXPERIMENTAL SECTION

Materials. All materials were purchased from Sigma-Aldrich, U.K., unless stated otherwise.

Electrospinning Polyethylene Terephthalate Scaffold. Electrospun scaffolds were produced by dissolving polyethylene terephthalate (PET) in 1:1 trifluoroacetic acid (TFA):dichloromethane (DCM) (Fisher Chemicals, U.K.) to create a 10% (w/v) solution. The polymer solution was loaded into a syringe (20 mL), and an 18 gauge needle (BD Falcon, U.K.) was attached. The syringe was securely fitted to a syringe pump-driver (Harvard Apparatus Ltd., U.K.). The needle tip was positioned 15 cm from a grounded steel collector plate. The PET solution was delivered at a constant flow rate of 0.5 mL/hour at 14 kV for 4 h. The scaffolds were air-dried in a fumehood for 24 h to allow residual solvent to evaporate.

Propagation of Epithelial Cells and Fibroblasts. The epithelial (Calu-3) and fibroblast (MRC-5) cell lines (LGC Standards cell, U.K.) were routinely cultured at 37 °C and 5% CO_2 in DMEM-F12 Ham or MEM media, respectively. Both culture media were supplemented with fetal calf serum (FCS) (10% (v/v)), L-glutamine solution (2 mM) (1% (v/v)), and an antibiotic/antimycotic solution (1% v/v) comprised of penicillin (10 000 units/mL), streptomycin sulfate (100 mg/mL), and amphotericin B (25 μg/mL).

Generation of Dendritic Cells. Dendritic cells (DC) were generated from peripheral blood monocytes as we have previously described. Briefly, peripheral blood mononuclear cells were isolated from human blood buffy coat (National Blood Transfusion Service, U.K.) using Histopaque density gradient centrifugation. Monocytes were isolated using CD14+ magnetic beads (Milteny Biotech, U.K.) to the purity of >98%.[13,24] Purified monocytes were cultured with GM-CSF (50 ng/mL) and IL-4 (250 IU/ml) (R&D Systems) for 6 days to generate immature DCs. DC phenotype was determined by flow cytometry after staining for cell surface markers including CD11c, CD83, CD83, and HLA-DR.[25]

Assembly of Epithelial–Fibroblast Cocultures. Electrospun scaffolds were cut to a size of 2 cm^2 and sterilized by irradiating with ultraviolet (UV) light at a distance of 8 cm for 15 min each side. The scaffolds were sterilely transferred to a 12 well culture plate and a steel ring was placed on top to secure the scaffold before further sterilization in an antibiotic/antimycotic solution overnight (37 °C, 5% CO_2). The sterilizing solution was removed and the scaffold washed with PBS before submerging the scaffold in the appropriate cell culture media to precondition the scaffold. Calu-3 and MRC-5 cells were inoculated inside of the steel ring onto separate PET scaffolds at a density of 3×10^5 cells/scaffold (1×10^6 cells/mL in 300 μL) and incubated for 72 h (37 °C, 5% CO_2) (Figure 1A).

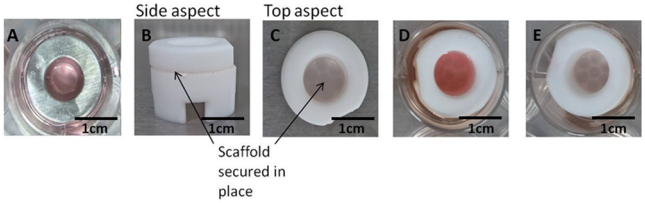

Figure 1. Steel rings are used to submerge the electrospun scaffolds and define the cell seeding area (A). The use of ScaffHolders (B–E) allow the 3D tissue engineered constructs of lung tissue to be cultured under appropriate conditions where epithelial cells are at the ALI (E) and fibroblast cells remain submerged, mimicking in vitro lung conditions.

Following 72 h culture, single culture scaffolds were transferred from steel rings into a polytetrafluoroethylene (PTFE) platform support (ScaffHolder), which was designed and fabricated in-house (Figure 1B–D). The epithelial scaffold monolayer was placed on top of the fibroblast scaffold layer inside the ScaffHolder to form the coculture model. This layer-on-layer approach is described in Figure 2. Single culture

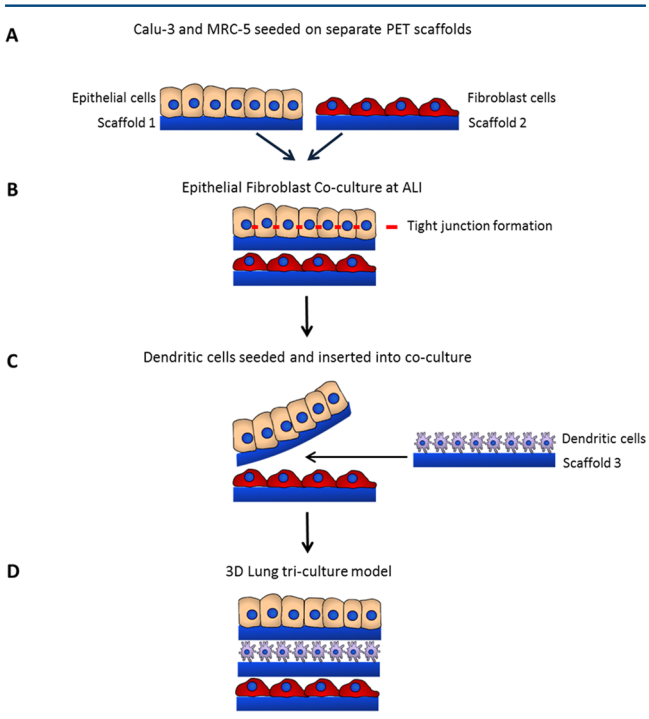

Figure 2. Schematic figure showing different steps of fabrication and configuration of the 3D tissue engineered airway epithelium. Calu-3 epithelial cells are seeded onto one PET scaffold and MRC-5 fibroblasts are seeded onto a second, separate scaffold (A). Following 72 h culture, scaffolds are combined by layering the epithelial scaffold monolayer on top of the fibroblast scaffold layer to form the coculture model. Cells are subsequently cultured for 2 weeks at the ALI to allow for differentiation of the epithelial cells, including establishment of tight junctions (B). Monocyte-derived DCs are seeded onto separate PET scaffolds and then inserted into the coculture model. The upper epithelial scaffold is temporally lifted away from the lower MRC-5 fibroblast layer so that the separate third scaffold containing dendritic cells may be placed on-top of the MRC-5 scaffold layer (C). The Calu-3 layer is placed on-top of the DC scaffold layer, resulting in the DC layer sandwiched between the epithelial and fibroblast scaffold layers to form the triculture model (D).

controls were assembled by combination of either a Calu-3 or MRC-5 scaffold with an acellular scaffold (i.e., without cells). To ensure there is no possibility of separation or movement during culture, scaffolds are secured in place within the ScaffHolder. Alignment of cell layers is ensured because the internal diameter of the steel ring matches that of the ScaffHolder (Figure 1). The cells were submerged in cell media for a further 12 h; the cell media for cocultures comprised a 50:50 mixture of the MRC-5 and Calu-3 cell media. Media from the apical surface of the ScaffHolder was removed to culture epithelial cells at the ALI (Figure 1E).

Assembly of Epithelial–Dendritic–Fibroblast Tri-Cultures. Epithelial–fibroblast cocultures were assembled and cultured for 14 days at the ALI prior to insertion of the DC

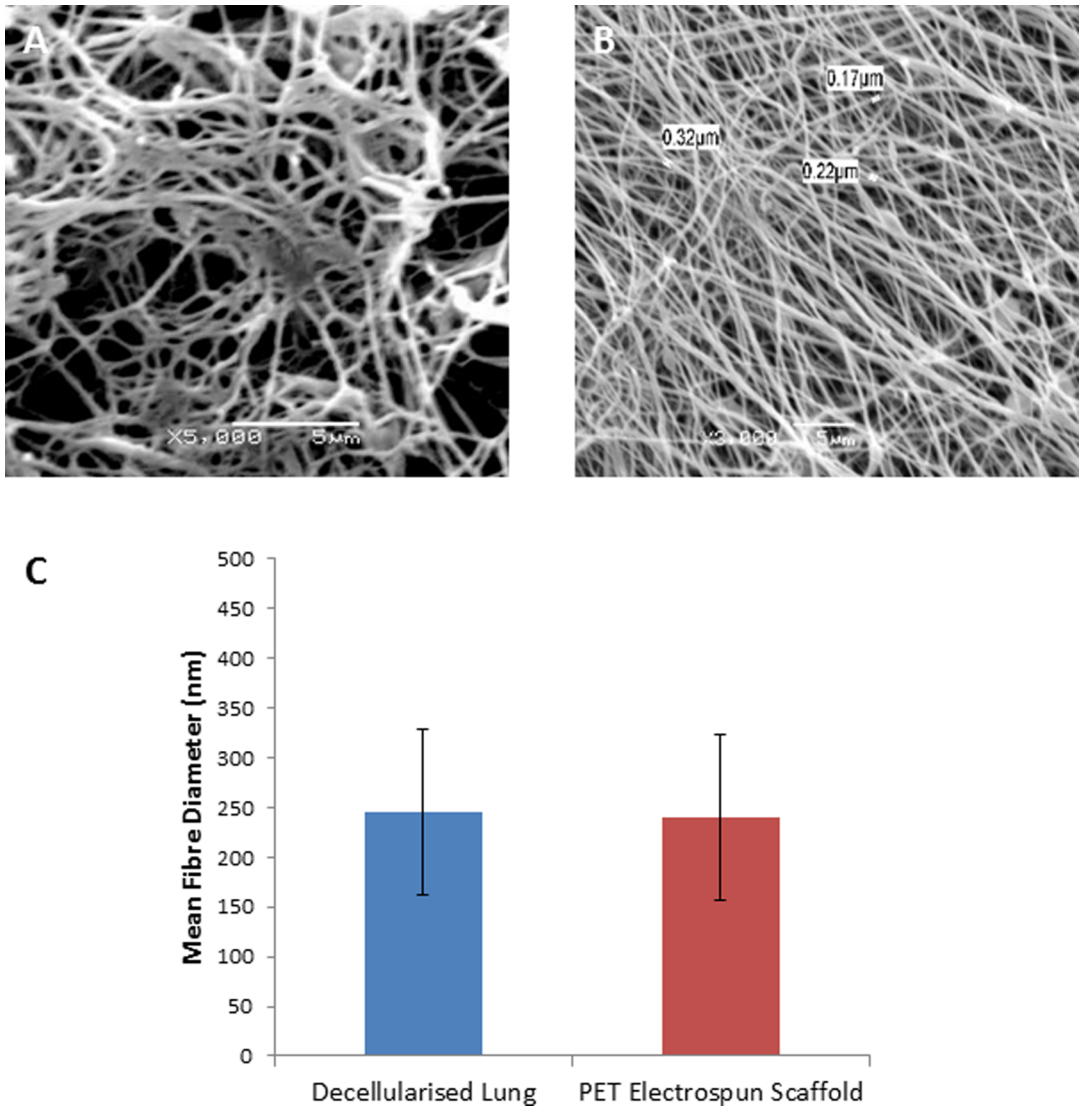

Figure 3. Comparisons of scanning electron micrographs of decellularised lung tissue (A) with PET electrospun scaffold (B) showing morphological similarities. The fiber diameter of decellularised lung tissue and PET electrospun scaffolds were measured and show comparable dimensions (C).

layer. The cell culture media composition remained as a 50:50 mixture of Calu-3 and MRC-5 cell media.

Immature DCs (Day 6) were prestained with Hoescht nuclear stain (5 μg/mL) (Invitrogen, U.K.) and inoculated onto PET electrospun scaffolds at a density of 2×10^5 cells/scaffold and incubated for 24 h (37 °C, 5% CO_2). The culture medium was aspirated to remove DCs that had not attached prior to insertion in between Calu-3 and MRC-5 layers in an established coculture model to form an immunocompetent triculture model. A schematic describing the layer-on-layer approach to assembling epithelial and fibroblast cocultures and subsequent insertion of the DC layer is described in Figure 2.

Stimulation of Triculture Model. Triculture models were stimulated with house dust mite extract (HDM) (10 μg/mL) (GREER, U.S.A.) and lipopolysaccharide (LPS) (100 ng/mL) (Sigma-Aldrich, U.K.) or PBS control and incubated for 36 h prior to analysis. The triculture models were fixed with 4% (v/v) paraformaldehyde (Electron Microscopy Sciences, U.S.A.) in PBS, and the three scaffold layers were separated and immunostained with pancytokeratin (epithelial cell marker). Scaffolds were then examined by confocal microscopy (Leica SP2 confocal laser scanning microscope) (Leica Microsystems Ltd., U.K.) with postvisualization performed using Volocity software (Perkin-Elmer, U.K.).

Trans-Epithelial Electrical Resistance Measurements. Trans-epithelial electrical resistance (TEER) measurements were performed across the epithelial cell monolayer of cells cultured at the ALI. Measurements were performed using an EVOM volt-ohm-meter and STX2 chopstick electrodes (World Precision Instruments, U.K.). Prior to recording TEER, chopstick electrodes were sterilized (70% v/v ethanol in distilled water) and cell culture media was added to the upper chamber (500 μL) and lower chamber (1.5 mL total volume) and allowed to equilibrate for 30 min (37 °C, 5% CO_2). Control measurements were performed using acellular scaffolds.

Scanning Electron Microscopy. Cellular samples of PET electrospun scaffold were placed onto carbon-coated electron microscope stubs and sputter-coated with gold (5 min, Blazers SCD 030 Blazers Union Ltd., Liechtenstein) under an argon atmosphere (BOC, U.K.) prior to analysis. Samples were imaged using SEM (Scanning Electron Microscopy) analysis (JEOL JMS-6060 LV microscope, JEOL Ltd., U.K.) operating at an accelerating voltage of 10 kV. Cellular samples were fixed

dx.doi.org/10.1021/mp5000295 | *Mol. Pharmaceutics* 2014, 11, 2082−2091

in 3% (v/v) glutaraldehyde overnight at 4 °C before dehydration through an ascending series of ethanol concentrations prior to SEM imaging.

Scaffold Histology. Histology preparation was performed by Nottingham University Advanced Microscopy Unit (AMU). Briefly, cellular scaffolds were fixed with 10% buffered formalin, excised, and embedded in paraffin. The paraffin embedded blocks were then sectioned and stained with hematoxylin and eosin (H&E) before imaging.

Immunocytochemistry. Scaffold samples were washed with PBS prior to fixation with paraformaldehyde (4% (w/v)) or methanol (100% (v/v)) for 15 min at room temperature (RT). Samples were washed in PBS (3 × 5 min each) before being permeabilized using Triton X-100 (0.5% (v/v)) for 5 min at room temperature. Following a further wash in PBS (3 × 5 min each), nonspecific antibody binding was blocked with goat serum (10% (v/v) in PBS for 5 min at room temperature. Samples were incubated with primary antibody (1:100) overnight at 4 °C. Primary antibodies used were Anti-Mucin 5AC [45M1] (ab3649, AbCam, U.K.), mouse anti-ZO1 (Invitrogen, U.K.), anti-fibronectin (ab 23750, AbCam, U.K.), Anti-Ki67 (ab15580, AbCam, U.K.), anti-collagen (ab34710, AbCam, U.K.), and pan-cytokeratin PK110 (SantaCruz Biotech, U.K.). Samples were then washed with PBS (3 × 5 min each) and incubated with species-appropriate fluorescently labeled secondary antibodies (1:100) for 30 min at room temperature. Secondary antibodies included goat antimouse IgG Rhodamine Red X (Invitrogen, U.K.), goat antirabbit IgG FITC (Invitrogen, U.K.), and Alexa Fluor 488 goat antimouse IgM (μ chain) (Invitrogen, U.K.). Samples were washed in PBS (3 × 5 min each), incubated with Hoechst (5 μg/mL) for 5 min at room temperature, and mounted using Fluoromount mounting medium. Immunostaining was observed using a confocal microscope (Leica SP2 confocal laser scanning microscope, images processed with Leica confocal software) with postvisualization performed using Volocity software.

Application of Papain. A papain (60U/mL) solution was prepared with L-cysteine (5 mM) to reconstitute the cysteine active site, and an aliquot (300 μL) was applied to the apical surface of Calu-3 cells. TEER measurements were performed to monitor epithelial barrier integrity prior and post application.

RESULTS

The present study presents a multilayered 3D electrospun PET lung model capable of incorporating multiple cell types each supported upon their own individual electrospun layer. The porous network of electrospun PET fibers can permit cell interaction through both direct cell−cell contact and paracrine factors within the 3D model. We report the incorporation of lung associated epithelial cells and fibroblasts and monocyte-derived DCs within the 3D model and determine how culturing these cells together influences their behavior.

Assembly of 3D Coculture Lung Model. SEM analysis of decellularised human lung tissue (from healthy sections of lung tissue obtained from patients undergoing surgical procedures (Nottingham University Hospitals NHS Trust) after informed consent and ethics approval) revealed a porous network of nanometer-sized fibers (Figure 3A). Accordingly, we used a nonbiodegradable polymer (namely, PET) to fabricate a nanoscale porous scaffold (Figure 3B). The mean fiber diameter of the PET scaffold (240 nm ±70) was similar to the mean diameter of lung ECM (245 nm ±83) (Figure 3C). The average thickness of the PET scaffold, calculated using histological sections, was 60 ± 10 μm. Owing to its robust physical properties, the PET electrospun scaffold is capable of withstanding repeat handling allowing separation of individual cell layers for assessment following experimentation.

The main structural cell types of the lung, epithelial, and fibroblast cells were each cultured upon separate PET scaffolds. To incorporate an immune component into the model, a triculture system was formed by culturing DCs upon a third PET scaffold and inserting this between the epithelial and fibroblast layers of an established epithelial−fibroblast coculture (Figure 2).

Epithelial Barrier Formation and Integrity. Epithelial and fibroblast cells were each inoculated onto individual PET scaffold layers and cultured submerged in media to allow cells to establish growth upon the scaffold, following which the cell inoculated scaffolds were assembled together within our developed ScaffHolders allowing physiologically relevant positioning of the construct. Epithelial cells were cultured upon the uppermost layer allowing culture at ALI where the upper cell surface is in contact with the air. Culturing epithelial cells at the ALI mimics in vivo conditions by providing apical−basal polarity, which leads to full differentiation of epithelial cells and development of a functional barrier.[26] The underlying fibroblasts were positioned directly beneath the epithelial inoculated scaffold and remained submerged in media much as they would in vivo.

The production and maintenance of barrier integrity in epithelial cells cultured upon PET electrospun scaffolds and positioned at the ALI using ScaffHolders was assessed using TEER measurements and permeability studies. Barrier formation was compared when epithelial cells were cultured alone (single culture) or with fibroblasts (coculture). TEER is widely used to monitor barrier integrity, where an increase in resistance to flow of current is due to greater integrity of the barrier, attributed to the formation of cellular tight junctions.[27]

An acellular control scaffold was monitored in order to report a control value, as it is known that TEER values reportedly vary according to the material upon which the epithelial cells are cultured.[28] In addition, a single culture of MRC-5 fibroblasts was monitored as a control, as an increase in TEER value was not expected owing to MRC-5 fibroblasts characteristically not forming tight junctions.

Statistical analysis was performed using two-way ANOVA with Sidàks multiple comparison showed that TEER measurements of cocultures produced readings that were significantly greater than those of epithelial cells cultured alone (Figure 4A).

The TEER measurements show that after 14 days in culture epithelial cells cultured alone, without fibroblasts, attained measurements of ∼130 Ω cm^2. The greatest increase was seen for cocultures of epithelial and fibroblast cells attaining measurements of ∼200 Ω cm^2. Thus, epithelial cells cultured together with fibroblasts appeared to achieve a confluent differentiated state earlier than single cultures of epithelial cells as shown by earlier and greater increases in TEER measurements (Figure 4 A). The TEER values of the controls, an acellular scaffold and MRC-5 single culture, did not increase, maintaining baseline TEER measurements of ∼100 Ω cm^2. Although human lung ex vivo TEER results are not available in the literature, ex vivo rabbit airway epithelium has been reported to be 260−320 Ω cm^2 for the trachea[29] and 266 Ω cm^2 for the bronchus.[30] Thus, the maximal TEER recorded in our 3D model are comparable to the data available for animal ex vivo TEERs.

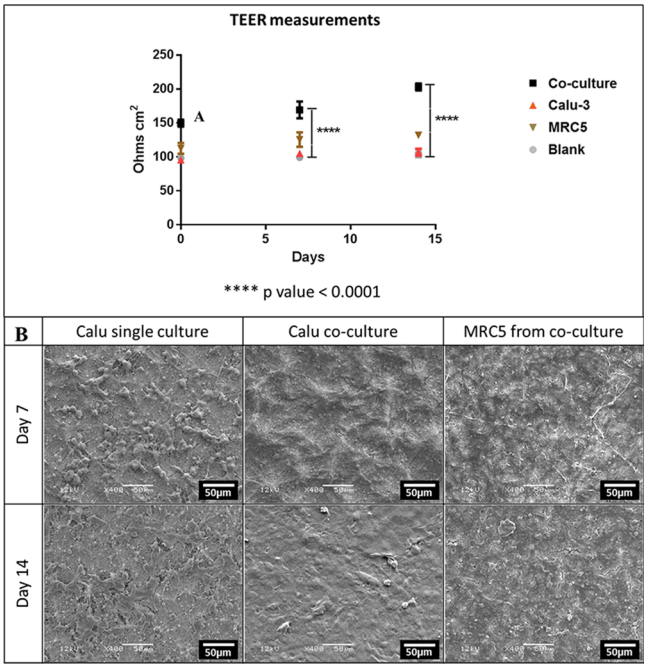

Figure 4. The TEER measurements of cocultures are significantly higher than those of epithelial cells cultured alone. Error bars show standard error of the mean. Statistical analysis was performed using two-way ANOVA with Sidaks multiple comparison with the difference between coculture and single Calu-3 culture having a p value <0.0001 (A). SEM images of epithelial cells from single and coculture where the upper surface that has been imaged is thought to be predominantly formed from ECM protein presence. The micrographs show that epithelial cells from coculture have a smoother surface than those from single culture (B).

The topography of the confluent epithelial cell layer was observed using SEM. The SEM micrographs of epithelial cells from single culture, coculture, and fibroblasts from cocultures showed what is thought to be the presence of ECM protein deposition (Figure 4B).

H&E staining of the epithelial layer from single and cocultures indicated that single cultures formed a single thin layer of cells, whereas the cocultured epithelial cells had a more dense and layered arrangement after 14 days at ALI (Figure 5). Furthermore, epithelial cells within cocultures appeared to produce mucus earlier than single cultures as shown by immunocytochemical staining (Figure 5).

Immunocytochemical staining of the deposition of ECM proteins indicated that the epithelial cells deposit collagen and fibronectin when cultured upon PET electrospun scaffolds (Figure 6). There appeared to be enhanced production of these ECM proteins from cocultured epithelial cells. The expression of the cell proliferation marker Ki67 showed that epithelial cells in coculture had lower levels of Ki67, possibly indicating their tendency toward an earlier full differentiated state as also evidenced by an accelerated increase in TEER readings in cocultures compared with single cultures of epithelial cells (Figure 7A). Fibroblast cell growth has not been adversely affected when positioned beneath the epithelial cell layer during coculture experimentation; the fibroblast cells are still present and in a state of active growth as indicated by the production of Ki67 and have retained the ability to produce ECM proteins collagen and fibronectin (Figure 6).

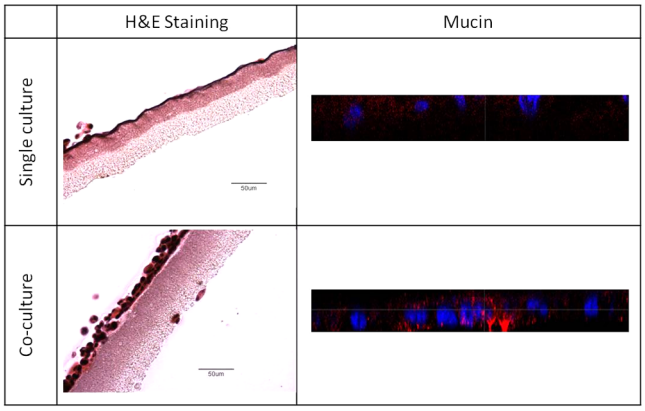

Figure 5. After 14 days at the ALI. Histological staining shows the presence of epithelial cells on the uppermost surface of the PET scaffold with a greater number of cells found in cocultures compared to single cultures. Mucin production (red) was greater from coculture than single culture, where cell nuclei are stained with DAPI (blue).

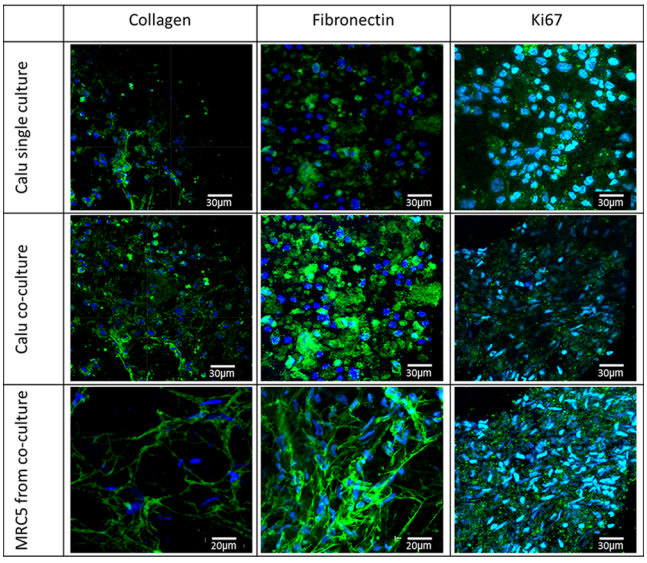

Figure 6. ECM staining following 14 days culture at the ALI shows the presence of ECM proteins: collagen and fibronectin, predominantly found in epithelial and fibroblast cells and also Ki67, showing that the cells are in active growth. Epithelial cells in cocultures appear to express lower levels of Ki67 (compared to single cultures), indicating their tendency toward full differentiation.

Epithelial Repair. The 3D lung model was cultured at the ALI for 14 days before papain was applied to the epithelial surface of single and cocultures. Papain is an allergen with cysteine protease activity and is known to disrupt tight junctions in respiratory epithelium using its enzymatic activity, mimicking the action of other airborne allergens such as house dust mite, which also have a cysteine protease activity.[31] The application of papain on day 14 ALI was shown to disrupt epithelial tight junctions in both single and coculture as demonstrated by a sharp reduction in TEER values (Figure 7A) and disintegration of ZO1 protein visualized by immunostaining followed by confocal imaging (Figure 7B). The disruption to tight junctions from coculture was thought to be less than that of single cultures, where almost no ZO1 could be observed post papain. TEER measurements were performed for a further 14 days to monitor the epithelial repair process, and further

dx.doi.org/10.1021/mp5000295 | Mol. Pharmaceutics 2014, 11, 2082−2091

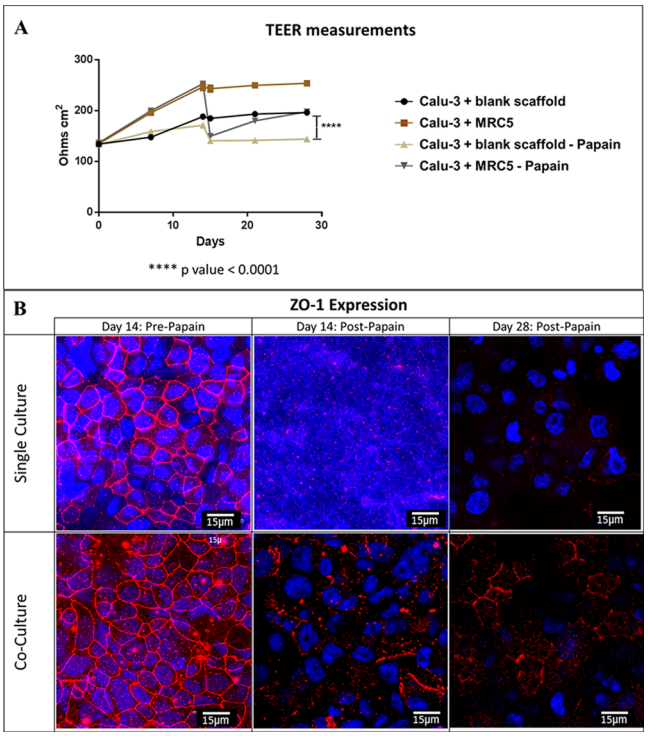

Figure 7. Following the 14 days at the ALI, the enzyme papain was applied to the epithelial surface of single and cocultures, which was shown to disrupt tight junctions demonstrated by the measurement of TEERs (A) and by confocal imaging of ZO1 protein (B). The disruption to tight junctions from coculture was observed to be less than that of single cultures. TEER measurements were then performed for a further 14 days to monitor the healing process. The cocultures were observed to be recovering from the disruption with increase in TEERS and increase in the presence of ZO1. Single cultures did not appear to recover so well with TEER measurements remaining around the same value as when the cells were subjected to papain. Statistical analysis was performed using two-way ANOVA with Sidaks multiple comparison, showing that the difference between coculture and single Calu-3 culture that had been subjected to papain having a p value <0.0001.

examination of ZO1 expression was carried out. The cocultures were observed to be recovering from the disruption with increased TEERS and increased presence of ZO1 (Figure 7A and B). However, TEER measurements did not appear to recover in single cultures during the same time frame and remained at approximately the same value as when the cells were subjected to papain (Figure 7A). The confocal microscopy images on day 15 (post papain) of single culture shows that the cell growth has been disrupted by papain and that tight junctions are not present over a wide area of the sample. The cells from single cultures recovered slightly as evidenced by the presence of nondisrupted nuclei on day 28; however, the presence of tight junctions remain absent (Figure 7B).

DC Migration within the 3D Triculture Model. In a proof-of-concept experiment, an immunocompetent triculture model comprising of epithelial, dendritic, and fibroblast layers was constructed and DC migration within the model monitored. The triculture model was stimulated with HDM extract (a common airborne allergen) and toll-like 4 receptor agonist LPS (abundant in most airborne bacterial pathogens), and subsequently, the migration of DCs was assessed by confocal microscopy. Epithelial cells were identified using pancytokeratin and DCs had been prestained using the nuclear stain Hoescht.[32] Assessment of the uppermost scaffold (bearing epithelial cells) revealed that after 36 h in the triculture, most DCs seemed to have migrated to this layer and were present in close proximity to the basal (in unstimulated samples) or apical side (in stimulated samples) of the epithelial cell layer (Figure 8A). The DCs migration was further confirmed by the fact that

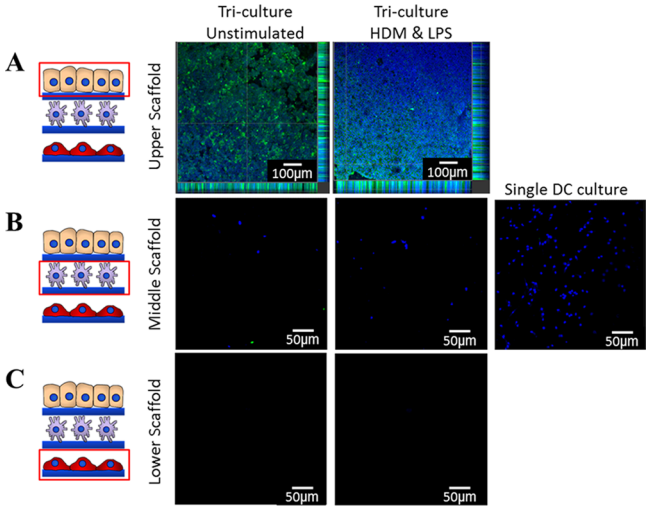

Figure 8. Confocal microscopy images (×10 mag) of DC migration 36 h after allergen stimulation in 3D tricoculture. The upper scaffold contained the Calu-3 epithelial layer (A), a middle layer to which DCs were seeded (B), and a lower scaffold containing MRC-5 (C). DCs were prestained with Hoescht nuclear stain (blue) and Calu-3 cells were poststained with pancytokeratin (green). In single culture, DCs remained on the middle scaffold where they had been inoculated. In the triculture, most DCs migrated from middle scaffold (B) to upper scaffold (A). Upon treatment of the triculture with house dust mite extract (HDM) (10 μg/mL) and lipopolysaccharide (LPS) (100 ng/mL), DCs appeared to primarily migrate to the apical surface of the epithelial layer, whereas in unstimulated samples they appear to be mainly localized in the basal region of the epithelial layer (A). Experiments were performed in duplicates.

DCs were found to be largely absent from the scaffold upon which they were originally inoculated (middle scaffold) (Figure 8B). Typically, not many DCs could be observed in the majority of lower scaffolds (fibroblast layer) in either stimulated or unstimulated samples (Figure 8C).

DISCUSSION

Using electrospun porous fibers, we have engineered a 3D triculture of airway epithelial cells, dendritic cells, and fibroblasts at ALI creating a modular construct that mimics the cellular orientation and some functional properties of human airway epithelium. The epithelium in vivo provides the first line of defense against environmental insults, and as such, it is capable of rapidly repairing any cellular damage caused. Epithelial cells in vivo are thought to respond to insult and injury through a cascade of events of which there are three distinct stages: dedifferentiation, proliferation, and differentiation.[33] The first stage is the dedifferentiation of underlying stromal cells, such as fibroblasts, that are initially exposed to the environment following injury to epithelial cells. The stromal cells are thought to migrate to the wound site to assist repair by dedifferentiation helping to cover the site of injury and assist in restoring barrier integrity through proliferation.[34] The final

dx.doi.org/10.1021/mp5000295 | Mol. Pharmaceutics 2014, 11, 2082−2091

stage in restoring barrier integrity is the differentiation of cells involved in the repair process, including the restoration of full function to epithelial cells, particularly their ability to form junctional protein to "seal" the barrier.[35]

The exact mechanisms controlling cell fate during epithelium repair are not clear; however, it is thought that multiple paracrine factors and direct cell−cell contact are key parameters required to restore barrier integrity and function.[36] It is, therefore, important to consider these factors when configuring tissue engineering strategies to create in vitro models of epithelial tissue.[36b]

This study developed a 3D multicellular lung model that is capable of forming a more physiologically relevant representation of lung tissue than culturing cells alone or in 2D systems. Our studies corroborate the relevance of culturing multiple cell types found in lung tissue together, as results demonstrate that when epithelial cells were subjected to chemical insult (i.e., an enzymatically active allergen), they recovered earlier in cocultures than single cultures. This supports the relevance of cocultures as it is thought that the cells signal and respond in alliance.

This study also assembled a triculture model in a proof-of-concept experiment to examine whether DC migration could occur within the lung model following stimulation.

A large number of DCs were found to migrate from the scaffold in which they were initially inoculated (middle layer) through to the uppermost scaffold bearing the epithelial cells. This occurred both in the presence and absence of stimulation and may suggest that DCs were responding to epithelial secretions.[37] However, in samples stimulated with LPS and HDM, most DCs were located closer to the apical side of the epithelial barrier, whereas in unstimulated samples they were mainly located close to the basal side. These results prove that the 3D lung model is amenable to cell migration and that cell−cell contact is feasible. Individual scaffolds are typically 60 ± 10 μm thick and the results of the DC migration study demonstrate that scaffold thickness does not seem to impede DC migration. The pattern of migration observed in this experiment substantiates DC migration in vivo, where upon activation, DCs migrate to the epithelium and survey the immune environment before migrating through the subepithelial compartment before traveling to lymph nodes.[7,37,38] This enables future studies focused on inhaled drug delivery systems as well as allergen and inhaled drugs uptake by DCs. We would estimate the triculture would be limited to one week due to migration of DCs and their phenotypical/functional changes upon stimulation, which should provide enough time for performing drug uptake/delivery experiments. Limitations to in vitro models, particularly those generated from commercially available 2D inserts, are that the surface upon which cells grow is planar, so cell−cell interaction is restricted. Cell interactions can occur through the pores of the insert; however, these are thought to be constrained to paracrine interactions because the pore size of the substrate upon which the epithelial cells are commonly cultured to allow barrier formation are too small, thus preventing cell migration. A 3D human skin triculture model comprising of keratinocytes, DCs, and fibroblasts has been reported.[14] This model shares similarities with the model developed in this work, including a physiologically relevant arrangement of the cell layers each supported on separate 3D scaffolds and the establishment of a differentiated epithelial−fibroblast coculture prior to DC insertion. In the skin triculture model, the keratinocytes and fibroblasts were supported on 3D microfiber-scale scaffolds; however, the DC layer was inserted into the model in an agarose gel rather than on a fibrous scaffold. Migration of DCs in the skin model was reported from the agarose gel layer to only the fibroblast layer. Furthermore, the degree of migration appeared to be far less than that observed in the 3D model developed in this study. Hence, direct seeding of DCs on the porous scaffolds as opposed to encapsulation within a hydrogel seems to facilitate cell migration.

Epithelial cell lines such as Calu-3, the cell line we have used in this study, are widely used as surrogates for primary cells.[39] Despite many similarities between Calu-3 and primary cells, particularly in features like barrier formation and mucus production, there are also considerable functional differences (e.g., their cytokine profile). Therefore, use of cell lines somewhat limits the physiological relevance of the model and future efforts should focus on replacing cell lines with human primary cells.

The 3D immunocompetent lung model presented in this study successfully supports the culture of multiple cell types on electrospun PET scaffolds that structurally resemble the native lung ECM. The porous network of electrospun PET fibers can permit cell interaction through both direct cell−cell contact and through paracrine factors within the 3D model as shown by the enhanced formation of a differentiated epithelial layer, enhanced epithelial repair, and migration of immune cells incorporated within the model. Furthermore, the modular nature of our approach means that other relevant structural (e.g., smooth muscle cells) and immune cells (e.g., mast cells or eosinophils) could be included into the model with relative ease.

Collectively, we believe this model possesses adequate cellular and structural representation of the airway epithelium and is amenable to in situ monitoring; as such, it presents an invaluable tool for academic and pharmaceutical research within the fields of lung biology, disease modeling, and drug discovery and delivery with the potential of reducing the need for some animal experimentation in this area.

AUTHOR INFORMATION

Corresponding Author

*A. M. Ghaemmaghami. Address: Division of Immunology, West Block, A Floor, Queen's Medical Centre, University of Nottingham, NG7 2UH, United Kingdom. E-mail: amg@nottingham.ac.uk.

Notes

The authors declare no competing financial interest.

ACKNOWLEDGMENTS

This work was jointly supported by a BBSRC Industrial Partnership Award (IPA) and Kirkstall Ltd (http://kirkstall.org) (BB/H011293/1).

ABBREVIATIONS

ALI, air−liquid interface; DC, dendritic cells; DCM, dichloromethane; ECM, extracellular matrix; FCS, fetal calf serum; HDM, house dust mite; LPS, lipopolysaccharide; PET, poly(ethylene terephthalate); PTFE, polytetrafluoroethylene; TEER, transepithelial electrical resistance; TFA, trifluoroacetic acid; UV, ultraviolet

REFERENCES

(1) Idoyaga, J.; Steinman, R. M. SnapShot: Dendritic Cells. *Cell* **2011**, *146* (4), 660−660 e2.

(2) Seok, J.; Warren, H. S.; Cuenca, A. G.; Mindrinos, M. N.; Baker, H. V.; Xu, W.; Richards, D. R.; McDonald-Smith, G. P.; Gao, H.; Hennessy, L.; Finnerty, C. C.; Lopez, C. M.; Honari, S.; Moore, E. E.; Minei, J. P.; Cuschieri, J.; Bankey, P. E.; Johnson, J. L.; Sperry, J.; Nathens, A. B.; Billiar, T. R.; West, M. A.; Jeschke, M. G.; Klein, M. B.; Gamelli, R. L.; Gibran, N. S.; Brownstein, B. H.; Miller-Graziano, C.; Calvano, S. E.; Mason, P. H.; Cobb, J. P.; Rahme, L. G.; Lowry, S. F.; Maier, R. V.; Moldawer, L. L.; Herndon, D. N.; Davis, R. W.; Xiao, W.; Tompkins, R. G. Inflammation; Host Response to Injury, L. S. C. R. P., Genomic responses in mouse models poorly mimic human inflammatory diseases. *Proc. Natl. Acad. Sci. U.S.A.* **2013**, *110* (9), 3507−12.

(3) (a) Ghaemmaghami, A. M.; Hancock, M. J.; Harrington, H.; Kaji, H.; Khademhosseini, A. Biomimetic tissues on a chip for drug discovery. *Drug Discovery Today* **2012**, *17* (3−4), 173−81. (b) Neuzi, P.; Giselbrecht, S.; Lange, K.; Huang, T. J.; Manz, A. Revisiting lab-on-a-chip technology for drug discovery. *Nat. Rev. Drug discovery* **2012**, *11* (8), 620−32.

(4) Ryu, J. H.; Kim, C. H.; Yoon, J. H. Innate immune responses of the airway epithelium. *Mol. Cells* **2010**, *30* (3), 173−83.

(5) Zhang, S.; Smartt, H.; Holgate, S. T.; Roche, W. R. Growth factors secreted by bronchial epithelial cells control myofibroblast proliferation: an in vitro co-culture model of airway remodeling in asthma. *Lab. Invest.: J. Tech. Methods Pathol.* **1999**, *79* (4), 395−405.

(6) (a) Bergeron, C.; Boulet, L. P. Structural changes in airway diseases: characteristics, mechanisms, consequences, and pharmacologic modulation. *Chest* **2006**, *129* (4), 1068−87. (b) Hammad, H.; Lambrecht, B. N. Dendritic cells and airway epithelial cells at the interface between innate and adaptive immune responses. *Allergy* **2011**, *66* (5), 579−87.

(7) Hammad, H.; Chieppa, M.; Perros, F.; Willart, M. A.; Germain, R. N.; Lambrecht, B. N. House dust mite allergen induces asthma via Toll-like receptor 4 triggering of airway structural cells. *Nat. Med.* **2009**, *15* (4), 410−6.

(8) Nichols, J. E.; Niles, J.; Riddle, M.; Vargas, G.; Schilagard, T.; Ma, L.; Edward, K.; La Francesca, S.; Sakamoto, J.; Vega, S.; Ogadegbe, M.; Mlcak, R.; Deyo, D.; Woodson, L.; McQuitty, C.; Lick, S.; Beckles, D.; Melo, E.; Cortiella, J. Production and assessment of decellularized pig and human lung scaffolds. *Tissue Eng., Part A* **2013**, *19* (17−18), 2045−62.

(9) Carterson, A. J.; Honer zu Bentrup, K.; Ott, C. M.; Clarke, M. S.; Pierson, D. L.; Vanderburg, C. R.; Buchanan, K. L.; Nickerson, C. A.; Schurr, M. J. A549 lung epithelial cells grown as three-dimensional aggregates: alternative tissue culture model for Pseudomonas aeruginosa pathogenesis. *Infect. Immun.* **2005**, *73* (2), 1129−40.

(10) Ravindran, S.; Song, Y.; George, A. Development of three-dimensional biomimetic scaffold to study epithelial-mesenchymal interactions. *Tissue Eng., Part A* **2010**, *16* (1), 327−42.

(11) Liu, Y.; Rayatpisheh, S.; Chew, S. Y.; Chan-Park, M. B. Impact of endothelial cells on 3D cultured smooth muscle cells in a biomimetic hydrogel. *ACS Appl. Mater. Interfaces* **2012**, *4* (3), 1378−87.

(12) (a) Rimann, M.; Angres, B.; Patocchi-Tenzer, I.; Braum, S.; Graf-Hausner, U., Automation of 3D Cell Culture Using Chemically Defined Hydrogels. *J. Lab. Autom.* **2013**; (b) DeVolder, R.; Kong, H.-J. Hydrogels for in vivo-like three-dimensional cellular studies. *Wiley Interdiscip. Rev.: Syst. Biol. Med.* **2012**, *4* (4), 351−365.

(13) Garcia-Nieto, S.; Johal, R. K.; Shakesheff, K. M.; Emara, M.; Royer, P. J.; Chau, D. Y.; Shakib, F.; Ghaemmaghami, A. M. Laminin and fibronectin treatment leads to generation of dendritic cells with superior endocytic capacity. *PLoS one* **2010**, *5* (4), e10123.

(14) Chau, D. Y.; Johnson, C.; MacNeil, S.; Haycock, J. W.; Ghaemmaghami, A. M. The development of a 3D immunocompetent model of human skin. *Biofabrication* **2013**, *5* (3), 035011.

(15) Huang, Y. X.; Ren, J.; Chen, C.; Ren, T. B.; Zhou, X. Y. Preparation and properties of poly(lactide-co-glycolide) (PLGA)/nano-hydroxyapatite (NHA) scaffolds by thermally induced phase separation and rabbit MSCs culture on scaffolds. *J. Biomater. Appl.* **2008**, *22* (5), 409−32.

(16) Ekaputra, A. K.; Prestwich, G. D.; Cool, S. M.; Hutmacher, D. W. Combining electrospun scaffolds with electrosprayed hydrogels leads to three-dimensional cellularization of hybrid constructs. *Biomacromolecules* **2008**, *9* (8), 2097−103.

(17) Harrington, H.; Rose, F. R. A. J.; Aylott, J. W.; Ghaemmaghami, A. M. Self-reporting Scaffolds for 3-Dimensional Cell Culture. *J. Visualized Exp.* **2013**, No. 81, e50608.

(18) (a) Matthews, J. A.; Wnek, G. E.; Simpson, D. G.; Bowlin, G. L. Electrospinning of collagen nanofibers. *Biomacromolecules* **2002**, *3* (2), 232−8. (b) Shih, Y. R.; Chen, C. N.; Tsai, S. W.; Wang, Y. J.; Lee, O. K. Growth of mesenchymal stem cells on electrospun type I collagen nanofibers. *Stem Cells* **2006**, *24* (11), 2391−7. (c) Rho, K. S.; Jeong, L.; Lee, G.; Seo, B. M.; Park, Y. J.; Hong, S. D.; Roh, S.; Cho, J. J.; Park, W. H.; Min, B. M. Electrospinning of collagen nanofibers: effects on the behavior of normal human keratinocytes and early-stage wound healing. *Biomaterials* **2006**, *27* (8), 1452−61.

(19) Wnek, G. E.; Carr, M. E.; Simpson, D. G.; Bowlin, G. L. Electrospinning of Nanofiber Fibrinogen Structures. *Nano Lett.* **2002**, *3* (2), 213−216.

(20) Intranuovo, F.; Howard, D.; White, L. J.; Johal, R. K.; Ghaemmaghami, A. M.; Favia, P.; Howdle, S. M.; Shakesheff, K. M.; Alexander, M. R. Uniform cell colonization of porous 3-D scaffolds achieved using radial control of surface chemistry. *Acta Biomater.* **2011**, *7* (9), 3336−44.

(21) (a) Cortiella, J.; Nichols, J. E.; Kojima, K.; Bonassar, L. J.; Dargon, P.; Roy, A. K.; Vacant, M. P.; Niles, J. A.; Vacanti, C. A. Tissue-engineered lung: an in vivo and in vitro comparison of polyglycolic acid and pluronic F-127 hydrogel/somatic lung progenitor cell constructs to support tissue growth. *Tissue Eng.* **2006**, *12* (5), 1213−25. (b) Bashur, C. A.; Dahlgren, L. A.; Goldstein, A. S. Effect of fiber diameter and orientation on fibroblast morphology and proliferation on electrospun poly(D,L-lactic-co-glycolic acid) meshes. *Biomaterials* **2006**, *27* (33), 5681−8. (c) Blackwood, K. A.; McKean, R.; Canton, I.; Freeman, C. O.; Franklin, K. L.; Cole, D.; Brook, I.; Farthing, P.; Rimmer, S.; Haycock, J. W.; Ryan, A. J.; MacNeil, S. Development of biodegradable electrospun scaffolds for dermal replacement. *Biomaterials* **2008**, *29* (21), 3091−104.

(22) (a) Telemeco, T. A.; Ayres, C.; Bowlin, G. L.; Wnek, G. E.; Boland, E. D.; Cohen, N.; Baumgarten, C. M.; Mathews, J.; Simpson, D. G. Regulation of cellular infiltration into tissue engineering scaffolds composed of submicron diameter fibrils produced by electrospinning. *Acta Biomater.* **2005**, *1* (4), 377−385. (b) Zhang, Y.; Yang, F.; Liu, K.; Shen, H.; Zhu, Y.; Zhang, W.; Liu, W.; Wang, S.; Cao, Y.; Zhou, G. The impact of PLGA scaffold orientation on in vitro cartilage regeneration. *Biomaterials* **2012**, *33* (10), 2926−2935.

(23) Ma, Z.; Kotaki, M.; Yong, T.; He, W.; Ramakrishna, S. Surface engineering of electrospun polyethylene terephthalate (PET) nanofibers towards development of a new material for blood vessel engineering. *Biomaterials* **2005**, *26* (15), 2527−2536.

(24) Emara, M.; Royer, P. J.; Mahdavi, J.; Shakib, F.; Ghaemmaghami, A. M. Retagging identifies dendritic cell-specific intercellular adhesion molecule-3 (ICAM3)-grabbing non-integrin (DC-SIGN) protein as a novel receptor for a major allergen from house dust mite. *J. Biol. Chem.* **2012**, *287* (8), 5756−63.

(25) Sharquie, I. K; Al-Ghouleh, A.; Fitton, P.; Clark, M. R.; Armour, K. L.; Sewell, H. F.; Shakib, F.; Ghaemmaghami, A. M. An investigation into IgE-facilitated 752 allergen recognition and presentation by human dendritic cells. *BMC Immunol.* **2013**, *14* (54), No. 10.1186/1471-2172-14-54.

(26) (a) Kasper, M.; Singh, G. Epithelial lung cell marker: current tools for cell typing. *Histol. Histopathol.* **1995**, *10* (1), 155−69. (b) Pohl, C.; Hermanns, M. I.; Uboldi, C.; Bock, M.; Fuchs, S.; Dei-Anang, J.; Mayer, E.; Kehe, K.; Kummer, W.; Kirkpatrick, C. J. Barrier functions and paracellular integrity in human cell culture models of the proximal respiratory unit. *Eur. J. Pharm. Biopharm.* **2009**, *72* (2), 339−49.

(27) Zhang, M.; Kim, K. J.; Iyer, D.; Lin, Y.; Belisle, J.; McEnery, K.; Crandall, E. D.; Barnes, P. F. Effects of Mycobacterium tuberculosis on the bioelectric properties of the alveolar epithelium. *Infect. Immunol.* **1997**, *65* (2), 692−8.
(28) Nalayanda, D. D.; Puleo, C.; Fulton, W. B.; Sharpe, L. M.; Wang, T. H.; Abdullah, F. An open-access microfluidic model for lung-specific functional studies at an air-liquid interface. *Biomed. Microdevices* **2009**, *11* (5), 1081−9.
(29) Bhat, M.; Toledo-Velasquez, D.; Wang, L.; Malanga, C.; Ma, J. H.; Rojanasakul, Y. Regulation of Tight Junction Permeability by Calcium Mediators and Cell Cytoskeleton in Rabbit Tracheal Epithelium. *Pharm. Res.* **1993**, *10* (7), 991−997.
(30) Rojanasakul, Y.; Wang, L.-Y.; Bhat, M.; Glover, D.; Malanga, C.; Ma, J. H. The Transport Barrier of Epithelia: A Comparative Study on Membrane Permeability and Charge Selectivity in the Rabbit. *Pharm. Res.* **1992**, *9* (8), 1029−1034.
(31) Shakib, F.; Ghaemmaghami, A. M.; Sewell, H. F. The molecular basis of allergenicity. *Trends Immunol.* **2008**, *29* (12), 633−42.
(32) Metzgeroth, G.; Mantz, C.; Kuhn, C.; Schultheis, B.; Hehlmann, R.; Hastka, J. Reliable identification of small cell lung cancer in cytological specimens by immunocytology. *Onkologie* **2007**, *30* (6), 311−5.
(33) Shimizu, T.; Nishihara, M.; Kawaguchi, S.; Sakakura, Y. Expression of phenotypic markers during regeneration of rat tracheal epithelium following mechanical injury. *Am. J. Respir. Cell Mol. Biol.* **1994**, *11* (1), 85−94.
(34) Davies, D. E. The role of the epithelium in airway remodeling in asthma. *Proc. Am. Thorac. Soc.* **2009**, *6* (8), 678−82.
(35) Stripp, B. R.; Reynolds, S. D. Maintenance and repair of the bronchiolar epithelium. *Proc. Am. Thorac. Soc.* **2008**, *5* (3), 328−33.
(36) (a) Knight, D. Epithelium-fibroblast interactions in response to airway inflammation. *Immunol. Cell. Biol.* **2001**, *79* (2), 160−4. (b) Vrana, N. E.; Lavalle, P.; Dokmeci, M. R.; Dehghani, F.; Ghaemmaghami, A. M.; Khademhosseini, A. Engineering functional epithelium for regenerative medicine and in vitro organ models: a review. *Tissue Eng., Part B* **2013**, *19* (6), 529−43.
(37) Banchereau, J.; Steinman, R. M. Dendritic cells and the control of immunity. *Nature* **1998**, *392* (6673), 245−52.
(38) Cook, D. N.; Bottomly, K. Innate immune control of pulmonary dendritic cell trafficking. *Proc. Am. Thorac. Soc.* **2007**, *4* (3), 234−9.
(39) Ong, H. X.; Traini, D.; Young, P. M. Pharmaceutical applications of the Calu-3 lung epithelia cell line. *Expert Opin. Drug Delivery* **2013**, *10* (9), 1287−302.